Limits on Passivating Defects in Semiconductors: The Case of Si Edge Dislocations

Tzu-Liang Chan, D. West, and S. B. Zhang

Phys. Rev. Lett. **107**, 035503 — Published 13 July 2011

DOI: 10.1103/PhysRevLett.107.035503

Limits on passivating defects in semiconductors: the case of Si edge dislocations

Tzu-Liang Chan, D. West and S. B. Zhang
Department of Physics, Applied Physics, and Astronomy,
Rensselaer Polytechnic Institute, Troy, New York 12180, USA

By minimizing the free energy while constraining dopant density, we derive a universal curve that relates the formation energy (E_{form}) of doping and the efficiency of defect passivation in terms of segregation of dopants at defect sites. The universal curve takes the simple form of a Fermi-Dirac distribution. Our imposed constraint defines a chemical potential that assumes the role of "Fermi energy", which sets the thermodynamic limit on the E_{form} required to overcome the effect of entropy such that dopant segregation at defects in semiconductors can occur. Using Si edge dislocation as an example, we show by first-principles calculations how to map the experimentally measurable passivation efficiency to our calculated E_{form} using the universal curve for typical n- and p-type substitutional dopants. We show that n-type dopants are ineffective. Among p-type dopants, B can satisfy the thermodynamic limit, while improving electronic properties.

PACS numbers: 61.72.-y,73.20.Hb,88.40.H-

Unintentional impurities and growth defects, for example vacancies and grain boundaries, are typical imperfections in semiconductors [1]. By prolonged annealing and carefully controlled epitaxy in ultra-high vacuum, it is plausible to eradicate the great majority of imperfections. However, such procedures should be balanced against the time and cost for manufacturing semiconductor devices. In fact, this balance is becoming increasingly important as semiconductor electronics is moving towards next-generation materials based on earth-abundant elements and organics for which prolonged annealing or epitaxy may not be an option. Even for the current technology, there are also urgent needs for widespread applications of renewable energy sources, specifically, photovoltaic (PV) materials for solar energy. There is generally a trade-off in PV materials: low-cost technologies (organic cells, amorphous-Si) are low efficiency, whereas high-cost technologies (multi-layered AlGaAs and InAlP junctions) are high efficiency. The low efficiency is related to defect states in the band gap that trap photogenerated electrons and holes and recombine them as heat [2, 3]. A cost-effective solution is to fabricate defect-tolerant materials, *e.g.,* instead of eliminating the impurities and growth defects, the defects are passivated by adding dopants into the system.

For polycrystalline materials, grain boundaries are effective recombination centers for photo-generated electrons and holes [4]. Their geometries are highly strained [5] resulting in deep levels inside the band gap [6, 7]. One criterion for the choice of the dopant is that the passivated defects should become electronically invisible to carrier transport, for example by reconstruction or strain relief. Even if such a dopant can be found, however, there is still a fundamental question of whether the dopant can reach the defects. Since the defect density is typically low, an introduced dopant is much more likely to go to a location with a bulk-like bonding environment (a bulk site), instead of associating with a defect to achieve passivation (a defect site). In other words, there is a large entropic contribution to the free energy which acts against passivation. In order to overcome this entropic effect, the dopant must have much lower energy in the vicinity of the defect (relative to bulk).

In this paper, we focus on the second criterion, the thermodynamic limit on the relative formation energy (ΔE) required for dopant segregation at the defects. To describe the experimentally relevant process of doping followed by annealing, we derive an expression for the effective passivation(percentage of defects which are passivated by the dopant) within the canonical ensemble. Additionally, by imposing the constraint that the dopant concentration does not significantly alter the electronic properties of the host material, we establish a universal relationship between ΔE and the maximum passivation efficiency, κ_D^{max}. With detailed derivation to be presented later in this letter, we illustrate the relationship between $\Delta E/kT$ and κ_D^{max} in Fig. 1(a), which follows a Fermi-Dirac distribution characterized by a chemical potential μ_s. μ_s is a resultant of our imposed constraint on the system, and is an effective Fermi energy that acts as a demarcation line to separate effective and ineffective doping. As an explicit example of our theory, our case study deals with an edge dislocation (ED) in Si since Si and Ge with small-angle grain boundaries, consisting of a series of EDs, are candidates for low cost/high quality PV materials [8]. Using substitutional dopants as our passivation candidates, we calculate their ΔE using first-principles density functional theory(DFT), and depict the resultant connection between the dopants and their passivation efficiencies through the universal curve in in Fig. 1(a). We find that B not only has sufficiently favorable formation energy ($E_{\rm form}$) at the dislocation to overcome the effect of entropy, it can also make the electron trap originating from the dislocation shallower without creating a deep acceptor level.

In order to determine whether a dopant can be intro-

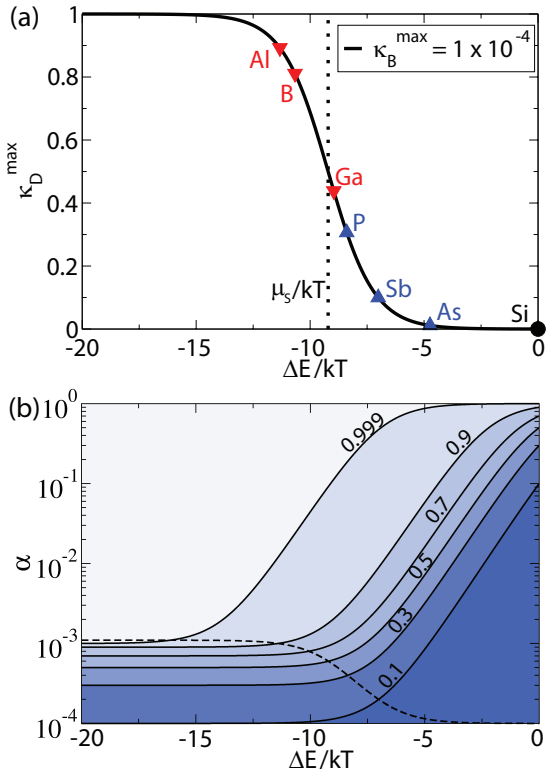

FIG. 1. (a) Maximum κ_D as a function of $\Delta E/kT$ is shown as a solid line. Shaded triangles (discussed later as a part of the DFT results) are a mapping between the various substitutional dopants in Si EDs and their κ_D^{max}, illustrated for T = 1100 K. (b) Contour plot of κ_D as a function of α and $\Delta E/kT$ for defect number density $\rho = 0.1\%$. The dashed line corresponds to the maximum possible α if the fraction of the occupied bulk sites is constrained to less than $\kappa_B^{max} = 1 \times 10^{-4}$. Intersection between the dashed line and contours defines the upper bound to κ_D (κ_D^{max}) as shown in (a).

duced and passivate defects, we should take both the E_{form} and entropy contribution into account. Given a fixed number of dopants n in the canonical ensemble, the equilibrium configuration corresponds to a minimum in free energy $F(n_D, n_B) = E_{form} - TS$, where $E_{form} = n_D E^D_{form} + n_B E^B_{form}$ is the total formation energy of the system. E^D_{form} and E^B_{form} represent the formation energy of the dopant substituted for a host atom at a defect site and substituted for a bulk site, respectively. The number of dopants at the defect sites n_D and those at the bulk sites n_B add up to n. The system has a total number of N sites, of which N_D (N_B) of them are defect (bulk) sites. The number of degenerate configurations with energy, E_{form}, is $\binom{N_D}{n_D}\binom{N_B}{n_B}$. At the minimum, $\Delta F = F(n_D + 1, n_B - 1) - F(n_D, n_B) = 0$. It follows that

$$\frac{\frac{\alpha}{\kappa_D} - \rho}{\frac{1-\alpha}{1-\kappa_D} - \rho} = exp(\frac{\Delta E}{kT}), \qquad (1)$$

where we have defined $\alpha = n/N$ as the dopant number density, $\rho = N_D/N$ as the defect number density, $\kappa_D = n_D/N_D$ as the passivation efficiency, and $\Delta E = E^D_{form} - E^B_{form}$ as the relative formation energy. In Fig. 1(b), we illustrate how κ_D varies with α and $\Delta E/kT$ for $\rho = 0.1\%$. The qualitative feature of the plot remains the same for other choices of ρ. Our goal is to push the passivation efficiency κ_D as close to 1 as possible. The figure depicts that if ΔE is not sufficiently negative, the only possible solution to push κ_D towards 1 is to push α towards 1. This is undesirable as the host material will become a degenerate semiconductor. Hence, Eqn. 1 should be solved with a constraint on the dopant number density for the bulk sites, $\kappa_B = \frac{n_B}{N_B} \leq \kappa_B^{max}$, which leads to a constraint on the total dopant number density, α. The accessible α is found to be constrained below the dashed line in Fig. 1(b). For a given $\Delta E/kT$, a specific value of the passivation efficiency κ_D is only possible if its corresponding contour line in Fig. 1(b) goes below the dashed line. Graphically, the intersection of the dashed line with the contour lines leads to a maximum possible passivation efficiency κ_D^{max} as a function of $\Delta E/kT$ as depicted in Fig. 1(a). To illustrate the trend, we set κ_B^{max} to be 1×10^{-4}, which is a doping concentration beyond which a semiconductor can be considered degenerate. Analytically, Eqn. 1 should be recast in a more convenient form:

$$-k\ ln\left(\frac{1}{\kappa_B} - 1\right) + k\ ln\left(\frac{1}{\kappa_D} - 1\right) = \Delta E/T. \qquad (2)$$

The first term on the left corresponds to the reduction in entropy after removing a dopant from a bulk site, and the second term is the subsequent gain in entropy when the dopant is then added to a defect site. Under the constraint $\kappa_B \leq \kappa_B^{max}$, it is straight forward to derive from Eqn. 2 that κ_D is bound from above by

$$\kappa_D \leq \kappa_D^{max} = \frac{1}{exp(\frac{\Delta E - \mu_s}{kT}) + 1}. \qquad (3)$$

Note that κ_D^{max} has a functional form of the Fermi-Dirac distribution with the chemical potential $\mu_s = -kT\ ln\left(\frac{1}{\kappa_B^{max}} - 1\right) \approx kT\ ln(\kappa_B^{max})$, which is the entropic change to the free energy by removing a dopant atom from the bulk sites when $\kappa_B = \kappa_B^{max}$. Hence, our imposed constraint leads to a chemical potential for the dopant atoms in the system, which determines the critical ΔE to overcome entropy. If ΔE is lower than μ_s, then dopant segregation to defects is highly effective, otherwise passivation of defects is nearly impossible. For $\kappa_B^{max} = 1 \times 10^{-4}$, $\mu_s = -9.21\ kT$. In the case of Si, the annealing temperature is typically above 1,100 K for dopant diffusion [16] at which $\mu_s = -0.88$ eV.

We considered typical n- (P, As, Sb) and p-type (B, Al, Ga) substitutional dopants in our study of the ED in Si. In order to determine ΔE and the electronic effects

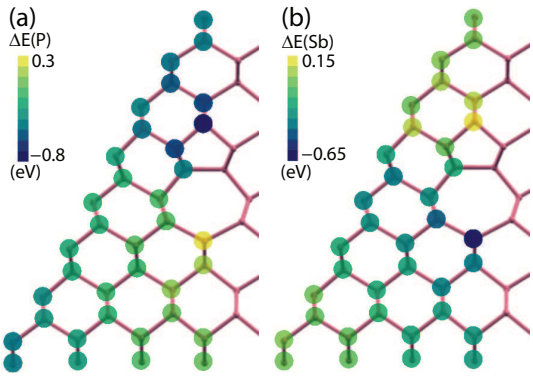

FIG. 2. (a) and (b) Position dependence of the ΔE for P and Sb around a Si ED along the $\langle 110 \rangle$ direction (normal to the page). The intensity of the color indicates the magnitude. Only half of the calculation unit cell is shown.

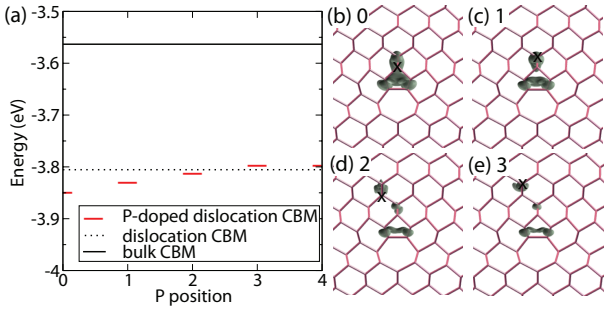

FIG. 3. (a) Evolution of the CBM as P moves away from the ED core, *i.e.* from position 0 to 4. The dislocation is along the axis of a hydrogen-passivated Si$\langle 110 \rangle$ nanowire. (b) to (e) Charge density contour plots for each P position. All the contour plots have the same charge density. The "x" denotes the position of the P.

of the various dopants, we performed first-principles calculations based on the density functional theory [9, 10] under the local density approximation. The exchange-correlation functional is from Ceperley and Alder [11] parametrized by Perdew and Zunger [12]. The calculations were performed using VASP (Vienna *ab initio* simulation package) [13]. Ultrasoft pseudopotentials [14, 15] are employed to replicate the ionic potentials. A plane wave cutoff of 15 Ryd is used. We checked that the difference in total energies between two structures is converged to within 0.01 eV for the chosen energy cutoff. Only the Γ point is used for the Brillouin zone integration. All the structures were minimized to a local energy minimum with forces on each atom less than 0.025 eV/Å. The atomic model consisting of linked five-fold and seven-fold rings is adopted for the ED [17]. An ED can be specified by the Burgers vector $\mathbf{b} = \frac{a}{2}(110)$ [5], where a is the lattice constant. As such, an isolated ED cannot be examined by periodic boundary condition. Instead, a dislocation dipole is employed in our studies such that the net Burgers vector from the two EDs cancel within the calculation unit cell [6]. The two EDs are separated by $\sim$ 12 Å. To ensure that the dopant does not interact with its periodic images, the periodicity along the $\langle 110 \rangle$ direction is set to be six times the primitive unit cell.

In Fig. 2(a), we depict ΔE for P on various Si sites in the vicinity of an ED. To obtain ΔE, we calculate E_{form} by $E+\mu(Si)-E_0-\mu(P)$, where E and E_0 are the total energy of the supercell with and without the dopant, respectively, and $\mu(P)$ ($\mu(Si)$) is the chemical potential of P (Si). We find that it is energetically favorable to substitute the Si at the tip of the five-fold ring of the ED by P. Dopants segregation to grain boundaries has also been found in similar studies [18–21].

For the case of P, the P-Si bond length is very similar to that of Si-Si in bulk. To elucidate the observed energetics, we examine the trend of the conduction band minimum (CBM) inside the Si energy gap as a function of P position in Fig. 3(a). Note here that the dislocation is a periodic line defect along the dislocation core. The "dislocation CBM" is the minimum energy ED trap originated from the bulk CBM. This study is carried out using a hydrogen-passivated Si$\langle 110 \rangle$ nanowire with an ED along the wire axis. While it has been suggested that LDA yields a too short distance for the interaction of the defect with the surface in nanowires[22, 23], here we are interested in bulk properties. Hence, we do not take into account the energetics of P on the nanowire surface where P segregation may occur.[24, 25] The use of a nanowire allows the electronic band structures between different calculations to be aligned more conveniently. From which, it can be seen that P is not a good candidate for passivation as it deepens the electron trap. Without the P dopant, there is an unoccupied electron trap associated with the ED within the Si energy gap [6] (represented by the dotted line in Fig. 3(a)), and the corresponding wave function is strongly localized on the five-fold ring. With the presence of an n-type P dopant, an electron is donated to the band inside the gap, which becomes partially occupied. Fig. 3(b-e) depict the charge density of the CBM with P at increasing distance from the dislocation. From (d) and (e), we can see the localization of the charge density around both the dislocation and P. This illustrates the competition between the P and the ED for the donor electron as it is energetically favorable for the electron to localize on both of them simultaneously. Consequently, the lowest energy configuration occurs when the P is at the five-fold ring (Fig. 3(b)), and the corresponding CBM is the lowest in energy. On the other hand, for the large n-type dopant Sb, the dopant-induced strain plays a significant role, and the lowest energy position is at the seven-fold ring of the ED where the Si bonds have tensile strain as illustrated in Fig. 2(b). Similarly, for p-type dopants the

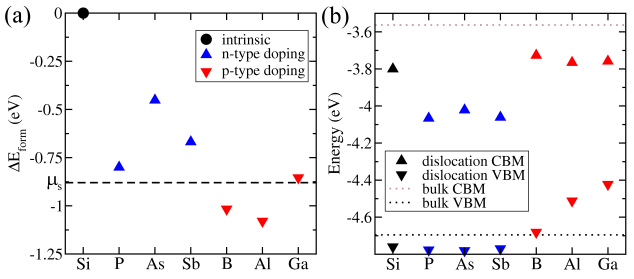

FIG. 4. The chemical trend of (a) the ΔE, (b) CBM and VBM of a doped Si ED in a hydrogen-passivated Si⟨110⟩ nanowire. In (a), the dashed line indicates the calculated chemical potential μ_s below which passivation is effective.

energetics is governed by strain. The lowest energy position for the small B is at the five-fold ring, where the Si bonds are compressed. Alternatively, Al and Ga are found at the seven-fold ring because of their larger sizes. For all the dopants considered, Fig. 4(a) shows that ΔE is negative. Fig. 1(a) depicts the maximum passivation efficiency κ_D^{max} for each dopant. It reveals that, despite $\Delta E < 0$, only p-type dopants (B, Al, and Ga) are thermodynamically attracted to Si EDs.

Fig. 4(b) depicts the VBM (valance band maximum) and CBM of a doped hydrogen-passivated Si⟨110⟩ nanowire with an ED along its axis. In order to assess the passivation effect of the dopants, we increased the dopant concentration such that there is one dopant for every two primitive unit cells along ED. Each dopant is at its lowest energy position. As a reference, the VBM and CBM of the undoped nanowire (with Si as the "dopant") are illustrated as well. The figure indicates that an ED without dopants is an electron trap as the CBM is inside the Si energy gap [6]. N-type doping results in the CBM sinking deeper into the gap. This can be understood in terms of the Coulomb attraction between the electron in the dislocation and the positive charge of the donor, which causes a lowering of the electrostatic potential at the ED and hence its lower gap level. P-type doping makes the CBM slightly shallower. It raises the VBM also when the size of the dopant is larger than Si. This can be understood in terms of the higher atomic p levels of the acceptors, causing hole localization. The best electronic dopant is B, which makes electron traps slightly shallower without introducing any deep acceptor level. For B doped p-type PV absorbers, dislocation traps will thus be less effective in causing non-radiative recombination, which is beneficial for the overall efficiency.

In conclusion, we derived a mapping between the formation energy of doping and the passivation efficiency. There is a universal thermodynamic limit on the formation energy such that introduced dopants can segregate at the defects while maintaining the electronic properties of the material. From the theoretical perspective, this allows one to quantitatively determine, from the calculated ΔE, which dopants can effectively passivate defects, while from the experimental perspective, this allows for the measurement of ΔE from κ_B,κ_D, and T via Eqn. 2. For passivating defects in low cost/high quality PV materials, we examined the passivation of EDs in Si by typical n- and p-type substitutional dopants. We found that n-type dopants are thermodynamically ineffective and electronically harmful as they tend to make the gap states of the EDs deeper. The most successful dopant in our study is B, which makes the electron trap shallower, while satisfying the thermodynamic criterion on the formation energy at the same time.

The work was supported by the U. S. Department of Energy, Office of Basic Energy Sciences under Contract No. DE-SC000262 and the Computational Materials Science Network (CMSN) program. Computational resources provided by the National Energy Research Scientific Computing Center (NERSC), and the Computational Center for Nanotechnology Innovations (CCNI).

[1] H. J. Queisser and E. E. Happer, Science **281**, 945 (1998).
[2] A. Goetzberger, C. Heblinga, and H.-W. Schock, Mat. Sci and Eng. Rep. **40**, 1-46 (2003).
[3] A. D. Compaan, Solar Energy Materials and Solar Cells **90**, 2170-2180 (2006).
[4] See, eg., Proc. of the IEEE Photovoltaic Specialists Conference 2010.
[5] C. Hammond, Introduction to Crystallography, Oxford University Press, USA; Revised edition (Nov. 12, 1992).
[6] F. Liu, *et al.*, Phys. Rev. B **51**, 17192 (1995).
[7] T. A. Arias and J. D. Joannopoulos, Phys. Rev. B **49**, 4525 (1994).
[8] C. Gaire, *et al.*, Nanotechnology **21**, 445701 (2010).
[9] P. Hohenberg and W. Kohn, Phys. Rev. **136**, B864 (1964).
[10] W. Kohn and L. J. Sham, Phys. Rev. **140**, A1133 (1965).
[11] D. M. Ceperley and B. J. Alder, Phys. Rev. Lett. **45**, 566 (1980).
[12] J. P. Perdew and Y. Wang, Phys. Rev. B **45**, 13244 (1992).
[13] G. Kresse and J. Furthmüller, Comput. Mat. Sci. **6**, 15-50 (1996);Phys. Rev. B **54**, 11169 (1996).
[14] D. Vanderbilt, Phys. Rev. B **41**, 7892 (1990).
[15] G. Kresse and J. Hafner, J. Phys.: Condens. Matter **6**, 8245 (1994).
[16] J. D. Plummer, M. D. Deal, and Peter B. Griffin, Silicon VLSI Technology, Prentice Hall, 2000.
[17] M. Mostoller, M. F. Chisholm, and T. Kaplan, Phys. Rev. Lett. **72**, 1494 (1994).
[18] T. A. Arias and J. D. Joannopoulos, Phys. Rev. Lett. **69**, 3330 (1992).
[19] A. Maiti, *et al.*, Phys. Rev. Lett. **77**, 1306 (1996).
[20] M. F. Chisholm, *et al.*, Phys. Rev. Lett. **81**, 132 (1998).
[21] T. Kaplan, *et al.*, Phys. Rev. B **61**, 1674 (2000).
[22] M. Diarra, *et al.*, Phys. Rev. B **75**, 045301 (2007).
[23] Y.M. Niquet, *et al.*, Phys. Rev. B **81**, 161301(R) (2010).
[24] R. Rurali, Rev. Mod. Phys. **82**, 427 (2010).
[25] M.V. Fernandez-Serra, Ch. Adessi, and X. Blase, Phys. Rev. Lett. **96**, 166805 (2006).